Investigation of NO and NO_2 Transformation in a Non-Thermal Plasma-Assisted SCR System with Cu/Al_2O_3

Pichitpon Neamyo[1,4],*Punya* Promhuad[2,4,*], *Warirat* Temwutthikun[2,4], *Sak* Sittichompoo[3,4], *Nuttapon* buntek[2], *Boonlue* Sawatmongkhon[3,4], *Thawatchai* Wongchang[1,4], and *Kampanart* Theinnoi[3,4]

[1]Department of Mechanical and Automotive Engineering Technology, Faculty of Engineering and Technology, King Mongkut's University of Technology North Bangkok (Rayong Campus), 21120 Rayong, Thailand
[2]KMUTNB Techno Park, King Mongkut's University of Technology North Bangkok, 10800 Bangkok, Thailand
[3]College of Industrial Technology, King Mongkut's University of Technology North Bangkok, 10800 Bangkok, Thailand
[4]Research Centre for Combustion Technology and Alternative Energy (CTAE), Science and Technology Research Institute, King Mongkut's University of Technology North Bangkok, 10800 Bangkok, Thailand

Abstract. This research investigates a hybrid methodology for the abatement of low-temperature NO_x by amalgamating non-thermal plasma (NTP) with a Cu/Al_2O_3 catalyst under conditions that simulate diesel exhaust. A catalyst consisting of 2 wt% Cu-loaded γ-Al_2O_3 was synthesized through the technique of incipient wetness impregnation and subsequently characterized using X-ray diffraction (XRD) and scanning electron microscopy with energy-dispersive X-ray spectroscopy (SEM–EDS), thereby confirming the presence of metallic Cu^0 and its uniform distribution. Plasma experiments were executed at input power levels of 20, 30, and 40 W. The results indicated that NTP in isolation effectively facilitated the oxidation of NO to NO_2, attributable to the generation of reactive species including O_3 and O*. Nevertheless, when this plasma treatment was employed in conjunction with the catalyst, both NO and NO_2 were concurrently eliminated via the rapid selective catalytic reduction (SCR) mechanism, resulting in substantially enhanced NO_x conversion rates. Further examination revealed that a reduction in the electrode gap resulted in an increase in electric field strength (E = V/d), which in turn amplified plasma reactivity. At a gap of 3 cm, the most significant NO_x reduction efficiency was attained due to improved NO oxidation and an optimal NO/NO_2 ratio entering the catalyst. In summary, this study elucidates that the efficacy of plasma-catalytic systems is influenced not solely by plasma power but also by the geometrical configuration of the reactor. These findings offer essential insights for the design of energy-efficient systems aimed at low-temperature NO_x control.

1 Introduction

Nitrogen oxides (NO_x), which predominantly include nitric oxide (NO) and nitrogen dioxide (NO_2), represent significant atmospheric contaminants primarily produced through combustion mechanisms in internal combustion engines [1]. Considerable emissions are also linked to external combustion sources, including coal- and gas-fired power generation facilities, industrial furnaces, and marine propulsion systems [2, 3]. These pollutants contribute to various environmental and public health concerns, encompassing acid precipitation, photochemical smog, the formation of ground-level ozone, and respiratory ailments [4, 5].

Selective Catalytic Reduction (SCR) has been extensively adopted as a proficient post-combustion technology for NO_x abatement, attaining substantial removal efficiencies under optimal thermal conditions (typically ranging from 250 to 400°C) [6, 7]. Nevertheless, SCR systems frequently experience diminished catalytic efficiency at lower temperatures, particularly during engine cold-start scenarios or during transient load conditions, wherein the reaction kinetics are adversely affected [8]. Furthermore, the necessity for ammonia or urea injection introduces the potential for ammonia slip, especially under conditions of suboptimal dosing or fluctuating thermal environments, which can result in secondary emissions and create the need for complex control strategies or supplementary catalysts (e.g., ammonia oxidation catalysts) [9].

To mitigate these constraints, Non-Thermal Plasma (NTP) technology has emerged as a promising solution for NO_x reduction at lower temperatures [10]. NTP systems harness energetic electrons generated during dielectric barrier discharges (DBDs) to initiate chemical transformations such as excitation, dissociation, and ionization without significantly elevating the overall gas temperature . A notably advantageous characteristic of NTP is its capacity to oxidize NO into NO_2, a more reactive species that plays a pivotal role in facilitating the rapid SCR pathway [11]:

* Corresponding author: punya.p@technopark.kmutnb.ac.th

$$NO+NO_2+2NH_3 \rightarrow N_2+3H_2O \quad (1)$$

The production of reactive oxygen and nitrogen species (RONS), encompassing O, O_3, OH•, and NO_3, further amplifies the oxidation mechanism and concurrently aids in the elimination of additional pollutants, including unburned hydrocarbons and soot [12, 13]. Nonetheless, systems utilizing only plasma commonly encounter obstacles, such as insufficient conversion of NO_x, the generation of unwanted byproducts (e.g., N_2O, O_3), and a comparatively elevated energy expenditure per unit of pollutant eliminated [14].

To mitigate these limitations, hybrid plasma–catalyst systems have been suggested, wherein plasma serves as an initial gas-phase activation phase preceding a catalytic reactor [15, 16]. Among the diverse array of catalytic supports, copper-loaded γ-alumina (Cu/Al_2O_3) has emerged as a subject of interest due to its considerable surface area, thermal resilience, and capacity to interact synergistically with species generated by plasma [17]. The integration of copper enhances redox activity, promotes the adsorption and activation of NO_x, and facilitates the breakdown of intermediates such as N_2O_5, thereby contributing to a more thorough reduction of NO_x [18].

Despite the promising prospects presented by plasma–catalyst systems, significant knowledge deficits persist concerning the influence of plasma operating parameters (e.g., power level) and reactor architecture (e.g., electrode gap distance) on the generation of reactive species and the subsequent selective catalytic reduction (SCR) process [19]. Specifically, the function of electric field strength (E = V/d) in modulating plasma density, energy transfer, and NO/NO_2 speciation remains inadequately elucidated, particularly under dynamically optimized catalytic conditions [20].

The objective of this investigation is to explore the synergistic effects of non-thermal plasma (NTP) and a Cu/Al_2O_3 catalyst on the reduction of NO_x under conditions simulating diesel exhaust. This research concentrates on (i) analyzing the impact of plasma power input on the conversion of NO to NO_2, (ii) evaluating the efficacy of the plasma–catalyst hybrid system in facilitating the rapid SCR mechanism, and (iii) investigating the influence of reactor geometry, specifically the electrode gap, on plasma reactivity and the overall efficiency of NO_x abatement. The findings are intended to furnish a mechanistic comprehension and practical insights for the optimization of plasma-assisted SCR technologies applicable to low-temperature emission control scenarios.

2 Experimental

2.1 Material preparation

A supported catalyst, comprising 2 wt% copper on γ-alumina, was synthesized utilizing the incipient wetness impregnation technique. The support material, γ-alumina (Ajax Finechem, Australia), exhibited a specific surface area of 142 m²/g, as evaluated by the Brunauer-Emmett-Teller (BET) methodology. The copper precursor, copper nitrate (Thomas Baker Chemicals, India), was solubilized in a minimal quantity of distilled water (0.5 cm³). This aqueous precursor solution was subsequently introduced meticulously to 1 g of the support material. The resultant sample was then subjected to drying in an oven at 110 °C overnight to eliminate the solvent. The final catalyst was achieved following calcination in static air at a temperature of 600°C for a duration of 2 hours, facilitating the decomposition of the nitrate precursor and the formation of the copper oxide phase.

2.2 Materials characterization

The crystalline phases of the synthesized catalytic materials were determined through the application of X-Ray Diffraction (XRD) methodologies. Data acquisition was performed utilizing a Rigaku Miniflex 600 diffractometer, which operates utilizing Cu-Kα radiation (λ = 1.5418 Å). The XRD patterns were recorded within the 2θ range of 10° to 90° at a scanning rate of 2°/min. The surface morphology and elemental composition of the catalytic materials were investigated through the utilization of a ZEISS AURIGA Field Emission Scanning Electron Microscope (FE-SEM), which was integrated with an Oxford Instruments Energy-Dispersive X-ray (EDX) spectrometer to facilitate comprehensive elemental analysis.

2.3 Experimental setup

A laboratory-scale apparatus was developed to replicate the composition of diesel engine exhaust gas and to examine the reduction of NO_x utilizing a non-thermal plasma (NTP) reactor, succeeded by a catalytic converter. The schematic representation of the experimental setup is depicted in Figure 1. The system encompassed five principal components: gas mixing and delivery, preheating furnace, NTP reactor, catalytic converter, and exhaust gas analysis.

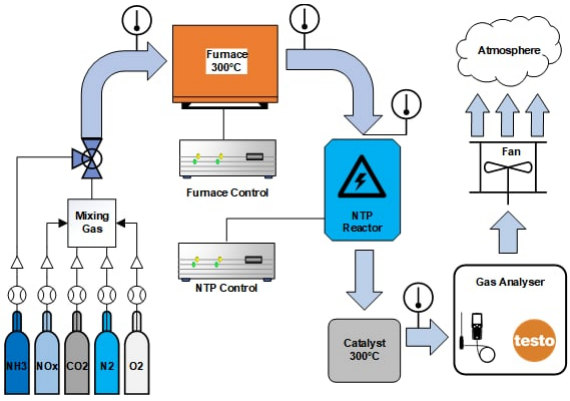

Fig. 1. Experimental configuration for plasma-assisted NO_x abatement utilizing non-thermal plasma (NTP) and a catalyst under conditions mimicking diesel exhaust.

The catalyst was packed in a quartz tube with an inner diameter of 0.5 inch (1.27 cm) and a bed height of 2 inches (5.08 cm), giving a geometric catalyst volume of approximately 6.4 cm³. At a total gas flow rate of 10

L/min (600 L/h, normalised at 25°C and 1 atm), the gas hourly space velocity (GHSV) was calculated as ~9.4 × 10^4 h^{-1}. This GHSV value was constant for all plasma power conditions.

High-purity gas cylinders containing ammonia (NH_3), nitrogen (N_2), carbon dioxide (CO_2), nitrogen oxides (NO_x), and oxygen (O_2) were utilized to replicate the composition of exhaust gases. The specifications for each gas were delineated as follows: O_2 (99.95%), N_2 (99.95%), CO_2 (99.95%), NH_3 (1,000 ppm in N_2), and NO_x (1,000 ppm in N_2). Each gas line was fitted with a flow meter and a unidirectional valve to ensure accurate flow regulation and to avert backflow. The gases were subsequently introduced into a stainless-steel mixing chamber, wherein a homogeneous mixing process transpired. The aggregate gas flow rate was meticulously maintained at 10 L/min, with the volumetric concentrations of each constituent adjusted to correspond with the simulated exhaust composition, as elaborated in Table 1.

Table 1. Simulated exhaust gas composition used for plasma–catalytic NO_x reduction experiments.

Gas species	Concentration	Unit
O_2	13.5	%
NOx	120.3	ppm
NO	114.8	ppm
NO_2	5.4	ppm
CO_2	6.0	%
NH_3	117.0	ppm

The mixed gas stream was subjected to preheating via an electric furnace to simulate the thermal conditions characteristic of engine exhaust. The temperature of the furnace was systematically monitored utilizing thermocouples and regulated through a digital furnace controller. The temperature metrics were exhibited on a digital temperature monitor to ascertain uniform inlet conditions for the NTP reactor. The exhaust temperature was sustained at approximately 300°C throughout the duration of the experiment, as this temperature is deemed optimal for SCR applications. The preheated gas was subsequently routed into the NTP reactor, which was designed in a Dielectric Barrier Discharge (DBD) configuration. The reactor was energized by an alternating current (AC) high-voltage source (220 V), with the input electrical energy meticulously monitored using a calibrated watt meter. An independent control unit was employed to modulate the operating voltage and frequency of the plasma discharge. Power discharges of 30, 40, and 60 W were administered to the NTP section to assess the impact of plasma energy on the efficiency of NO_x removal. After the plasma treatment, the gas stream traversed through a catalytic converter filled with the catalyst under investigation. The catalyst zone was additionally equipped with a thermocouple to monitor temperature during operation, thereby ensuring optimal conditions for catalytic NO_x reduction. The outlet gas stream was conditioned by a gas regulator and subsequently directed through a fan system prior to being released into the atmosphere. A TESTO 350 gas analyser was utilized to quantify the concentrations of NO_x and other gaseous species in real-time. The Testo 350 provides sufficient resolution and accuracy for exhaust gas analysis, with specifications as follows: O_2 (resolution 0.01 vol.%, accuracy ±0.2 vol.%), NO (resolution 1 ppm, accuracy ±5 ppm for 0–99 ppm and ±5% of reading for 100–1999 ppm), and NO_2 (resolution 0.1 ppm, accuracy ±5 ppm for 0–99.9 ppm and ±5% of reading above 100 ppm). All gas concentrations reported in Table 1 (O_2 13.5 vol.%, NO 114.8 ppm, NO_2 5.4 ppm, NH_3 117 ppm, CO_2 6.0 vol.%) are therefore above the instrument's resolution limits and within the stated accuracy range. The collected data were transmitted to a computer for logging and subsequent analysis. Outlet NH_3 concentration was monitored using a handheld NH_3 gas detector (0–1000 ppm range, 1 ppm resolution, accuracy ±3% F.S.). No NH_3 slip was detected under any experimental condition. All electrical devices, inclusive of the furnace and plasma control units, were powered by a 220–250 VAC electrical source. Power consumption for the NTP reactor was recorded using a watt meter for the purpose of evaluating energy efficiency.

The NOx mass flow rate was calculated from the measured concentration difference (ΔC, ppm) using the following equation:

$$\dot{m}_{NO_x} = \frac{P \cdot \dot{V}_{gas} \cdot \Delta C \cdot MW}{R \cdot T \cdot 10^6}$$

where P is the system pressure (1 bar), $\dot{V}_{gas}$ is the total volumetric flow rate of the feed gas (m^3 s^{-1}), ΔC is the NOx reduction in ppm (as NO_2 equivalent), MW is the molecular weight of NO_2 (46 g mol^{-1}), R is the universal gas constant (8.314 J mol^{-1} K^{-1}), and T is the absolute temperature (573 K). The calculated mass flow rate is expressed in g h^{-1}.

The specific NOx reduction, normalized to the plasma input power, was then obtained as:

$$\eta_{NO_x} = \frac{\dot{m}_{NO_x} \times 1000}{P_{in}}$$

where P_{in} is the plasma input power (W). The unit of η_{NOx} is g kWh^{-1}.

3 Result and Discussion

3.1 XRD Result

Figure 2 illustrates the X-ray diffraction (XRD) patterns corresponding to the Cu/Al_2O_3 catalyst. Distinct diffraction peaks attributable to both Cu and Al_2O_3 were detected. The existence of Cu was substantiated by its characteristic diffraction peaks observed at 2θ values of approximately 42° and 50°, which align with the standard diffraction pattern for metallic copper (Cu^0) as per JCPDS No. 04-0836 [21]. Moreover, distinctive peaks of Al_2O_3 were recognized at around 20°, 30°, 37°, 39°, 45°, 60°,

65°, 66°, and 79°, signifying the presence of the γ-Al_2O_3 phase as the support material [22].

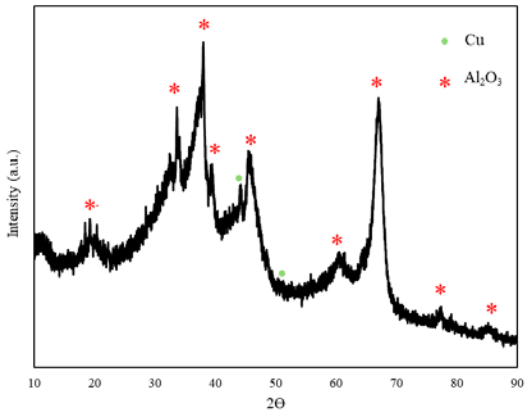

Fig. 2. XRD patterns of the Cu/Al_2O_3 catalyst indicating the presence of metallic Cu and γ-Al_2O_3 phases

The identification of metallic copper, in preference to copper oxide (CuO or Cu_2O), implies that the Cu species remain in a reduced state after the preparation of the catalyst, which is of considerable importance for redox reactions. Copper-based catalysts supported on γ-Al_2O_3 have been documented to play a pivotal role in facilitating the selective catalytic reduction (SCR) of NO_x with NH_3, particularly at low to moderate temperatures [23]. The well-dispersed Cu^0 species on the surface of Al_2O_3 significantly enhance electron transfer mechanisms and promote the interaction between NH_3 and NO_x, culminating in enhanced efficiency of NO_x conversion [24].

These observations corroborate the successful integration of Cu onto the Al_2O_3 support, which is essential for optimizing catalytic performance. The presence of crystalline Cu^0 further suggests robust thermal and structural stability under the prevailing reaction conditions, which will be elaborated upon in the subsequent section regarding NO_x reduction performance.

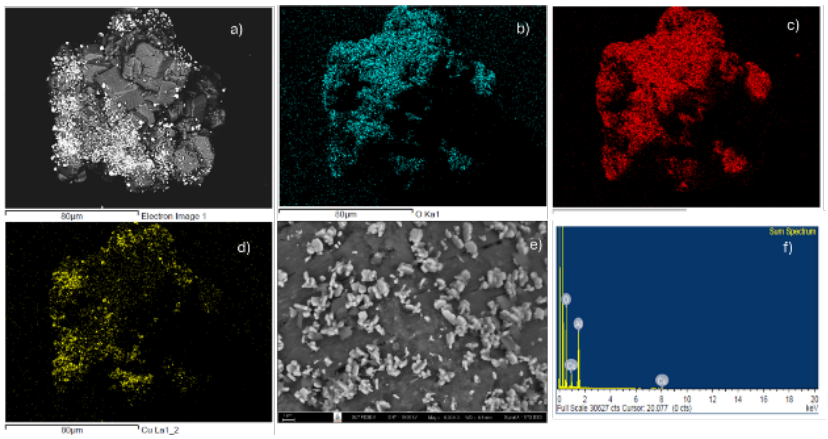

Fig. 3. SEM and EDS analyses reveal a uniform copper distribution on the γ-Al_2O_3 substrate. This finding confirms effective synthesis and supports enhanced NO_x reduction performance.

3.2 SEM-EDS Result

Figure 3 shows SEM micrographs and EDS mapping of the synthesized Cu/Al_2O_3 catalyst. Panel (a) presents the overall SEM image, while panels (b), (c), and (d) correspond to the EDS elemental mappings of oxygen (O), aluminum (Al), and copper (Cu), respectively. Panel (e) shows a higher magnification SEM image revealing surface morphology with well-dispersed particles, and panel (f) displays the EDS spectrum confirming the elemental composition.

The presence of oxygen and aluminum throughout the sample confirms the Al_2O_3 support, as also validated by the XRD peaks of γ-Al_2O_3 in Figure 2. Importantly, the EDS mapping in panel (d) shows that copper is evenly dispersed across the catalyst surface, without observable agglomeration. This observation is consistent with the XRD results in which metallic Cu^0 peaks were detected, suggesting successful incorporation of copper in its reduced form.

The high dispersion of copper is a critical factor for catalytic activity [25]. A uniform distribution of Cu species enhances the availability of active sites, promotes interaction with NO_x and NH_3, and improves the overall efficiency of the SCR process [26]. Moreover, the absence of copper oxide peaks in the XRD pattern and the fine dispersion in the EDS mapping both indicate that the synthesis method yields a high-quality catalyst with metallic Cu^0 well anchored on the Al_2O_3 surface.

This combination of XRD and EDS analyses strongly supports that the catalyst preparation was effective and that the resulting material possesses the structural and compositional features necessary for enhanced NO_x reduction performance under NTP-assisted conditions.

3.3 Analysis of NO and NO_2 Concentration under Different Power Conditions

As illustrated in Figure 4, the initial gaseous effluent exhibited concentrations of 114.82 ppm of nitrogen monoxide (NO) and 5.45 ppm of nitrogen dioxide (NO_2).

The introduction of a 20 W non-thermal plasma (NTP) resulted in a pronounced alteration in the concentrations of nitrogen oxides. The concentration of NO experienced a substantial decline, reducing to 46.00 ppm, which was concomitant with a marked elevation in the NO_2 concentration to 67.61 ppm. This finding underscores the significant oxidative potential inherent in the NTP environment. The conversion of NO to NO_2 can be attributed to reactions involving plasma-generated reactive oxygen species (ROS), predominantly atomic oxygen (O•) and ozone (O_3) [27]. These findings align with the following plasma-mediated reaction mechanisms [28]:

$$NO+O^* \rightarrow NO_2 \quad (2)$$
$$NO+O_3 \rightarrow NO_2 \quad (3)$$

In the case of Cu/Al_2O_3-only treatment (absent plasma influence), NO was reduced to 55.94 ppm while NO_2 remained undetectable at 0 ppm, signifying typical selective catalytic reduction (SCR) activity devoid of oxidative processes. When both NTP and Cu/Al_2O_3 were employed concurrently, NO further diminished to 39.00 ppm, and NO_2 was eliminated, indicating that plasma-generated NO_2 was rapidly consumed via the accelerated SCR reaction.

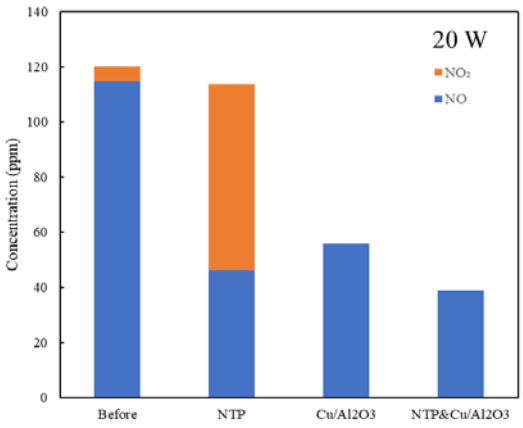

Fig. 4. Impact of solitary and synergistic applications of NTP and Cu/Al_2O_3 interventions on the concentrations of NO and NO_2 at a plasma power of 20 W.

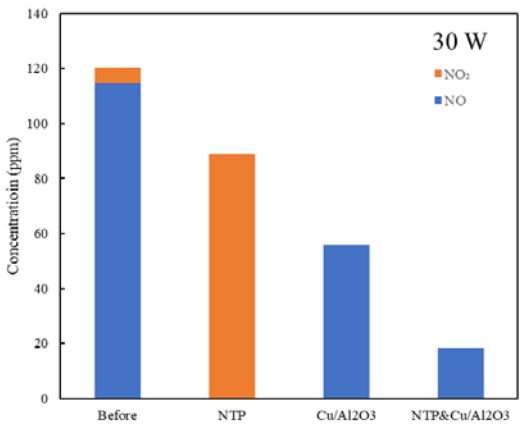

Fig. 5. Efficiency of NO oxidation and NO_x removal under 30 W plasma input with and without Cu/Al_2O_3 catalyst.

As illustrated in Figure 5, an escalation of the plasma power to 30 W significantly modified the reaction pathways. Under conditions exclusive to NTP, NO was completely oxidized to 0 ppm, resulting in a considerable increase in NO_2 concentration to 88.70 ppm. This observation signifies a heightened production rate of oxidizing species such as O• and O_3, which may subsequently lead to the formation of dinitrogen pentoxide (N_2O_5) through the ensuing reactions. Conversely, the catalyst-only system achieved a reduction of NO to 55.94 ppm without yielding any measurable NO_2. The synergistic effect of the combined NTP and Cu/Al_2O_3 system was markedly evident, as it drastically diminished NO concentration to 18.50 ppm while concurrently achieving complete removal of NO_2 (0 ppm). This reflects an exceptionally efficient conversion of NOx, which is ascribed to the facilitation of the rapid SCR mechanism, augmented by the presence of plasma-generated NO_2.

$$NO_2+O_3 \rightarrow NO_3+O_2 \quad (4)$$
$$NO_2+NO_3 \leftrightharpoons N_2O_5 \quad (5)$$

This transformation indicates that a fraction of NO_2 undergoes further oxidation to form N_2O_5 under conditions characterized by elevated ozone and high-energy plasma. Although N_2O_5 is not directly quantifiable via standard NO/NO_2 analysers, its generation signifies a transformation in NO_x speciation and may elucidate the observed minor discrepancy in NO_2 accumulation. Notably, N_2O_5 can also engage in NO reduction through reactions with ammonia (NH_3), thereby contributing to enhanced NO_x removal [29]:

$$N_2O_5+2NH_3 \leftrightharpoons N_2+3H_2O \quad (6)$$

This supplementary pathway offers an alternative route for plasma-assisted reduction, particularly in atmospheres abundant in ozone and ammonia. These reactions further augment the efficiency of NO_x abatement and exemplify the intricate interplay between plasma chemistry and catalytic activity. Consequently, the generation and subsequent degradation of N_2O_5 under non-thermal plasma conditions may contribute to the reduction of residual NO concentrations beyond conventional selective catalytic reduction pathways.

The influence of an elevated plasma power input of 40 W is illustrated in Figure 6. In the absence of a catalytic agent, the application of plasma treatment alone resulted in the total conversion of NO, thereby diminishing its concentration to 0 ppm. This phenomenon was accompanied by a pronounced increase in NO_2 concentration to 201.48 ppm, the peak level recorded, signifying that an excessive input of plasma energy facilitates extensive oxidation processes. Conversely, the Cu/Al_2O_3 catalyst demonstrated consistent performance under conditions of lower power, leading to a reduction of NO to 55.94 ppm.

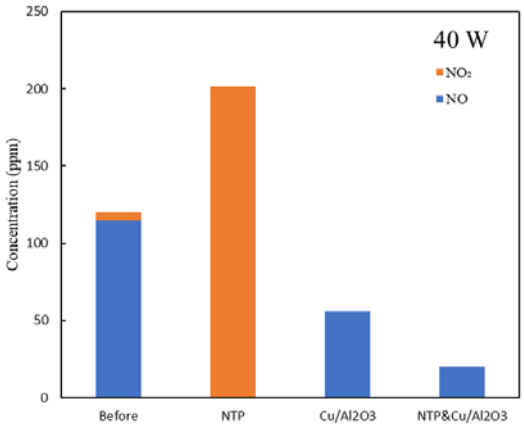

Fig. 6. Enhanced NO_2 formation and NO_x reduction by combined NTP and catalyst system at 40 W.

The synergistic capabilities of the hybrid system were most prominently observed under these experimental conditions. The integrated NTP + Cu/Al_2O_3 configuration achieved the minimal NO concentration at 25.38 ppm while simultaneously attaining complete elimination of NO (0 ppm). This observation suggests that the reactive oxidants, particularly NO_2, produced by the high-power plasma were effectively harnessed and consumed by the catalyst in the rapid selective catalytic reduction pathway, thereby reinforcing the collaborative interaction between the plasma- and catalyst-mediated reaction mechanisms. The pronounced increase in NO_2 concentration at 40 W can also be explained by the influence of the background gas composition. In the simulated exhaust, species such as O_2, N_2, CO_2, and NH_3 coexist with NO and NO_2. At sufficiently high plasma power, the energetic electrons promote additional dissociation of O_2 and partial excitation of N_2 These reactive species can subsequently participate in plasma-driven reactions, leading to further formation of NO and its oxidation to NO_2. For example, reactions between N_2 and O_2 under plasma excitation ($N_2 + O\bullet \rightarrow NO + N\bullet$, followed by $NO + O\bullet/O_3 \rightarrow NO_2$) can contribute significantly to the observed accumulation of NO_2. This synergistic effect explains why the highest NO_2 concentration was detected under NTP-only conditions at 40 W.

This trend became more pronounced at higher plasma wattages (30–40 W), where the increased discharge energy density intensified electron impact dissociation of O_2 molecules. As a result, larger amounts of reactive oxygen species (ROS), particularly atomic oxygen (O•) and ozone (O_3), were produced. These ROS accelerated the oxidation of NO into NO_2 through reactions (2) and (3), leading to a clear increase in NO_2 concentration under NTP-only conditions. In addition, at elevated wattages, a fraction of the formed NO_2 may undergo further oxidation to yield N_2O_5 in the presence of excess O_3. Although N_2O_5 was not directly detected by the analyser, its formation reflects a shift in NO_x speciation under high-energy plasma environments and further supports the explanation for the enhanced NO_2 accumulation observed.

When the Cu/Al_2O_3 catalyst was introduced, the change in NO with increasing NTP wattage can be explained by plasma–catalyst synergy. Higher discharge power intensifies electron-impact processes ($e^- + O_2 \rightarrow O\bullet + O\bullet + e^-$; $O\bullet + O_2 + M \rightarrow O_3 + M$), thus raising the flux of $O\bullet/O_3$ that oxidize NO to NO_2 ($NO + O\bullet/O_3 \rightarrow NO_2$). On the catalyst, Cu redox sites (Cu^{2+}/Cu^+) and the Al_2O_3 surface promote (i) NO oxidation via adsorbed O and nitrate/nitrite intermediates and (ii) SCR pathways once NH_3 is present in the feed. With increasing wattage, plasma-activated NH_3 (e.g., $NH_3 \rightarrow NH_2\bullet$) accelerates the surface steps of standard and fast SCR ($4NH_3 + 4NO + O_2 \rightarrow 4N_2 + 6H_2O$; $2NH_3 + NO + NO_2 \rightarrow 2N_2 + 3H_2O$), resulting in a net decrease of NO. At the highest wattage, competing side reactions (partial NH_3 oxidation to NO/NO_2, NO_2 decomposition, and site blocking by nitrate species) may moderate the net NO removal, yielding a plateau or slight rebound. Overall, the observed NO trend arises from the balance among plasma-phase NO oxidation, catalyst-mediated $NO \rightarrow NO_2$ and $NO \rightarrow N_2$ routes, and power-dependent side reactions.

To evaluate the energy performance of the system, the NOx mass flow rate (g/h) and the specific NOx reduction (g/kWh) were calculated based on inlet–outlet concentrations, flow rate, plasma input power, and the molecular weight of NOx (expressed as NO_2 equivalent). The results are presented in Table 2. As can be seen, the NTP-only case shows limited efficiency and even negative values at 40 W, confirming that plasma alone can promote NOx formation under high-energy conditions. In contrast, the NTP+Cu/Al_2O_3 configuration demonstrates much higher specific NOx reduction, with up to 2.36 g/kWh at 20 W, highlighting the synergistic effect between plasma activation and catalytic SCR pathways.

Table 2. Mass flow rate and specific NOx reduction under different plasma powers and operating conditions

Condition	Power (W)	Mass flow rate (g/h)	Specific NOx reduction (g/kWh)
NTP	20	0.0039	0.20
	30	0.0183	0.61
	40	-0.0470	-1.18
NTP+Cu/Al_2O_3	20	0.0471	2.36
	30	0.0590	1.97
	40	0.0550	1.38

3.4 Influence of Reactor Geometry on Plasma-Catalytic NO_x Reduction

The synergistic interaction between non-thermal plasma (NTP) and selective catalytic reduction (SCR) was rigorously examined by manipulating the electrode gap of the reactor while maintaining a constant plasma power output of 40 W. As elucidated in Figure 7 and Table 2, the spatial configuration of the plasma discharge region exerted a significant effect on the overall efficiency of NO_x reduction within the integrated system.

Table 3. Electrical Characteristics and Reactor Parameters at 40 W Plasm Power

Reaction Gap (cm)	Discharge Voltage (kV)	E (kV/cm)
6	43.3	7.2
4	32.0	8.0
3	27.4	9.1

The findings illustrate a distinct inverse correlation between the electrode gap and the conversion rate of NO. Optimal performance was observed at the minimum gap of 3 cm, where the resultant outlet NO concentration was diminished to its lowest level of approximately 20 ppm. Conversely, as the gap was expanded to 4 cm and subsequently to 6 cm, the outlet NO concentration exhibited an increase to approximately 30 ppm and 45 ppm, respectively.

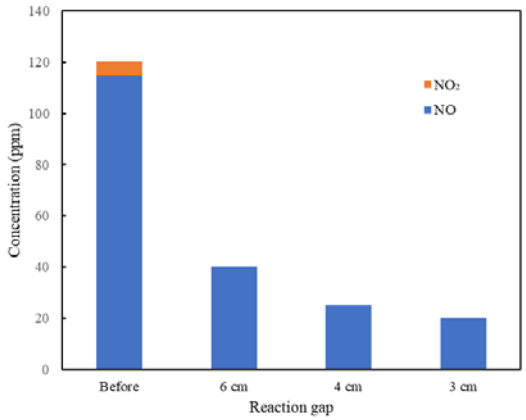

Fig. 7. The influence of reaction gap distance on the concentrations of NO and NO_2 during NTP operation at 40 W.

This observed pattern correlates directly with the strength of the electric field (E), which is determined by the equation E=V/d. Although the discharge voltage (V) experienced a reduction as the gap (d) was minimized, the resultant electric field exhibited a marked intensification, escalating from 7.2 kV/cm at a 6 cm gap to 9.1 kV/cm at a 3 cm gap. The augmented electric field facilitates the acceleration and energy of electrons, thereby enhancing the production rate of reactive oxygen and nitrogen species (RONS), including O•, O_3, and NO_3. The primary function of the plasma within this hybrid system is to effectively oxidize a fraction of the initial NO into NO_2. This plasma-generated NO_2 is essential for facilitating the highly efficient rapid SCR reaction on the subsequent Cu/Al_2O_3 catalyst. Consequently, the heightened plasma reactivity at the 3 cm gap establishes an optimal NO/NO_2 ratio that enters the catalyst bed, thereby maximizing the overall NO_x conversion. This observation underscores the critical importance of optimizing reactor geometry, not only for enhancing plasma performance but also for improving the synergistic efficacy of plasma-catalytic systems in the realm of pollution control.

4 Conclusion

This study demonstrates the effectiveness of a hybrid non-thermal plasma (NTP) and Cu/Al_2O_3 catalytic system for nitrogen oxides (NO_x) reduction at low temperatures resembling diesel exhaust conditions. A catalyst with 2 wt% Cu-loaded γ-Al_2O_3 was developed, showing highly dispersed metallic Cu^0 essential for enhancing selective catalytic reduction (SCR) activity. The combination of NTP and the catalyst created a synergistic mechanism utilizing plasma-generated oxidants with catalytic reduction processes. Adjusting the plasma input power revealed that NTP alone could efficiently oxidize nitric oxide (NO) to nitrogen dioxide (NO_2), with higher power levels (30–40 W) significantly increasing NO_2 production. However, when integrated with the Cu/Al_2O_3 catalyst, the generated NO_2 was rapidly consumed through SCR reactions, leading to superior NO_x conversion compared to individual treatments. The presence of intermediary species like N_2O_5 under high-energy plasma conditions further complicated and enhanced the plasma-assisted reaction network. Additionally, reactor geometry, specifically the electrode gap, was carefully analyzed. A smaller reaction gap (3 cm) produced the highest electric field intensity (9.12 kV/cm), increasing plasma reactivity and promoting NO oxidation, thus optimizing the NO/NO_2 ratio entering the catalytic zone. This condition achieved the lowest residual NO concentration (~20 ppm), underscoring the importance of geometric optimization for maximizing plasma–catalyst synergy. In conclusion, the results confirm that reactor design, plasma power adjustment, and catalyst integration are interconnected factors affecting NO_x reduction efficacy. These findings provide a scientific basis for advancing energy-efficient, low-temperature deNO_x technologies based on plasma-catalytic systems.

This research budget was allocated by National Science, Research and Innovation Fund (NSRF), and King Mongkut's University of Technology North Bangkok (Project No. KMUTNB-FF-68-B-26).

References

1. S. Meier, E.F.M. Koene, M. Krol, D. Brunner, A. Damm, G. Kuhlmann,A lightweight NO2-to-NOx conversion model for quantifying NOx emissions of point sources from NO_2 satellite observations, Atmos. Chem. Phys. 24, 7667–7686 (2024). https://doi.org/10.5194/acp-24-7667-2024
2. M.A. Gonzalez-Salazar, T. Kirsten, L. Prchlik, Review of the operational flexibility and emissions of gas- and coal-fired power plants in a future with growing renewables, Renewable and Sustainable Energy Reviews, 82 (2018) 1497–1513. https://doi.org/10.1016/j.rser.2017.05.278
3. Z. Ma, Y. Yang, P. Sun, H. Xing, S. Duan, H. Qu, Y. Zou, Analysis of marine diesel engine emission characteristics of different power ranges in China, Atmosphere, 12(9) (2021) 1108. https://doi.org/10.3390/atmos12091108

4. I. Manisalidis, E. Stavropoulou, A. Stavropoulos, E. Bezirtzoglou, Environmental and Health Impacts of Air Pollution: A Review, Frontiers in Public Health, 8 (2020) 14. https://doi.org/10.3389/fpubh.2020.00014
5. J. Sun, A.J. Barnes, D. He, M. Wang, J. Wang, Systematic Review and Meta-Analysis of the Association between Ambient Nitrogen Dioxide and Respiratory Disease in China, International Journal of Environmental Research and Public Health, 14(6) (2017) 646. https://doi.org/10.3390/ijerph14060646
6. G. Busca, L. Lietti, G. Ramis, F. Berti, Chemical and mechanistic aspects of the selective catalytic reduction of NOx by ammonia over oxide catalysts: A review, Applied Catalysis B: Environmental, 18(1–2) (1998) 1–36. https://doi.org/10.1016/S0926-3373(98)00040-X
7. S. Roy, M.S. Hegde, G. Madras, Catalysis for NOx abatement, Applied Energy, 86(11) (2009) 2283–2297. https://doi.org/10.1016/j.apenergy.2009.03.022
8. B. Guan, R. Zhan, H. Lin, Z. Huang, Review of state of the art technologies of selective catalytic reduction of NOx from diesel engine exhaust, Applied Thermal Engineering, 66(1–2) (2014) 395–414. https://doi.org/10.1016/j.applthermaleng.2014.02.021
9. M. Jabłońska, "Progress on noble metal-based catalysts dedicated to the selective catalytic ammonia oxidation into nitrogen and water vapor (NH3-SCO)," Molecules, vol. 26, no. 21, 6461, 2021, https://doi.org/10.3390/molecules26216461.
10. W. Temwutthikun, P. Promhuad, T. Iamcheerangkoon, B. Sawatmongkon, K. Theinnoi, S. Sittichompoo, An Experimental Investigation on Enhancing Nitrogen Oxides Reduction of Non-Thermal Plasma (NTP) Aftertreatment System with Silver-Base Catalyst with NTP Downstream SCR Catalyst Configuration. Materials Science Forum. (2024). https://doi.org/10.4028/p-CcFD5C
11. R. Gholami, C.E. Stere, A. Goguet, C. Hardacre, Non-thermal-plasma-activated de-NO_x catalysis, Philosophical Transactions of the Royal Society A: Mathematical, Physical and Engineering Sciences, 376(2110) (2018) 20170054. https://doi.org/10.1098/rsta.2017.0054
12. H. H. Kim, "Nonthermal plasma processing for air-pollution control: a historical review, current issues, and future prospects," Plasma Processes and Polymers, vol. 1, no. 2, pp. 91–110, 2004, https://doi.org/10.1002/ppap.200400028
13. M. Babaie, P. Davari, P. Talebizadeh, F. Zare, H. Rahimzadeh, Z. Ristovski, and R. Brown, "Performance evaluation of non-thermal plasma on particulate matter, ozone and CO_2 correlation for diesel exhaust emission reduction," Chemical Engineering Journal, vol. 276, pp. 240–248, 2015, https://doi.org/10.1016/j.cej.2015.04.086
14. S. Teodoru, Y. Kusano, and A. Bogaerts, "The effect of O_2 in a humid $O_2/N_2/NO_x$ gas mixture on NO_x and N_2O remediation by an atmospheric pressure dielectric barrier discharge," Plasma Processes and Polymers, vol. 9, pp. 652–689, 2012, https://doi.org/10.1002/ppap.201100187.
15. J. Van Durme, J. Dewulf, C. Leys, H. Van Langenhove, Combining non-thermal plasma with heterogeneous catalysis in waste gas treatment: A review, Applied Catalysis B: Environmental, 78(3–4) (2008) 324–333. https://doi.org/10.1016/j.apcatb.2007.09.035
16. H.-L. Chen, H.-M. Lee, S.-H. Chen, M.-B. Chang, S.-J. Yu, S.-N. Li, Removal of volatile organic compounds by single-stage and two-stage plasma catalysis systems: A review of the performance enhancement mechanisms, current status, and suitable applications, Environmental Science & Technology, 43(7) (2009) 2216–2227. https://doi.org/10.1021/es802679b
17. Y. Li, J. Su, J. Ma, F. Yu, J. Chen, and R. Li, "Novel straight synthesis of super-microporous Cu/Al2O3 catalyst with high CH4-SCR-NO activity," Catalysis Communications, vol. 65, pp. 6–9,2015, https://doi.org/10.1016/j.catcom.2015.02.020
18. K. Shimizu, H. Kawabata, H. Maeshima, A. Satsuma, and T. Hattori, "Intermediates in the selective reduction of NO by propene over Cu–Al2O3 catalysts: Transient in situ FTIR study," Journal of Physical Chemistry B, vol. 104, no. 13, pp. 2885–2893, 2000, https://doi.org/10.1021/jp9930705
19. V. Palma, M. Cortese, S. Renda, C. Ruocco, M. Martino, E. Meloni, A Review about the Recent Advances in Selected Nonthermal Plasma Assisted Solid–Gas Phase Chemical Processes, Nanomaterials, 10(8) (2020) 1596. https://doi.org/10.3390/nano10081596
20. J.T. Herron, Modeling studies of the formation and destruction of NO in pulsed barrier discharges in nitrogen and air, Plasma Chemistry and Plasma Processing, 21 (2001) 581. https://doi.org/10.1023/A:1012003218939
21. JCPDS-ICDD, Powder Diffraction File, Card No. 04-0836 (Cu), International Centre for Diffraction Data, Newtown Square, PA, USA.
22. S. Selpiana, D. N. Sari, E. Purwaningsih, Synthesis and characterization catalyst γ-Al_2O_3 and Al/γ-Al_2O_3, Indonesian Journal of Fundamental and Applied Chemistry, 7(1) (2022) 26–31. https://doi.org/10.24845/ijfac.v7.i1.26
23. J. Li, H. Chang, L. Ma, J. Hao, R.T. Yang, Low-temperature selective catalytic reduction of NOx with NH3 over metal oxide and zeolite catalysts—A review, Catalysis Today, 175 (2011) 147–156. https://doi.org/10.1016/j.cattod.2011.03.034
24. N. Jraba, T. Makhlouf, G. Delahay, H. Tounsi, Catalytic activity of Cu/η-Al_2O_3 catalysts prepared from aluminum scraps in the NH_3-SCO and in the

NH_3-SCR of NO, Environmental Science and Pollution Research, 29(6) (2022) 9053–9064. https://doi.org/10.1007/s11356-021-16206-1

25. M. Hattori, T. Hattori, M. Ozawa, The chemical state and Cu+ stability for three-way catalytic performance of Cu-added Al2O3 catalysts. (2023). https://doi.org/10.1016/j.apcata.2023.119515
26. B. Zhu et al., Insights into the active sites of copper species in CuO/SiO2 catalysts for NH3-SCR: Quantitative analysis and mechanism study. Fuel. (2024). https://doi.org/10.1016/j.fuel.2024.131341
27. P. Chonpan, K. Theinnoi, T. Iamcheerangkoon, P. Promhuad, S. Sittichompoo, Effects of operating parameters on dielectric barrier discharge non-thermal plasma ozone generator performance and NO Conversion. E3S web of conferences. **610**, 4001 (2025). https://doi.org/10.1051/e3sconf/202561004001
28. J. H. Bae, H. Lee, S.-C. Huh, S. Park, Nitric and Nitrous Acid Formation in Plasma-Treated Water: Decisive Role of Nitrogen Oxides (NO=1–3). Chemosphere. 143105 (2024). https://doi.org/10.1016/j.chemosphere.2024.143105
29. L. S. Ko, K. L. Pan, M. B. Chang, Deep oxidation of NO via catalytic ozonation. J Air Waste Manage Assoc.(2024). https://doi.org/10.1080/10962247.2024.2416047